Cluap1 is Essential for Ciliogenesis and Photoreceptor Maintenance in the Vertebrate Eye

Chanjae Lee,[1] John B. Wallingford,[1,2] and Jeffrey M. Gross[1]

[1]Department of Molecular Biosciences, Institute for Cellular and Molecular Biology, The University of Texas at Austin, Austin, Texas, United States
[2]Howard Hughes Medical Institute, The University of Texas at Austin, Austin, Texas, United States

Correspondence: Jeffrey M. Gross, 2401 Speedway, Austin, TX 78712, USA; jmgross@austin.utexas.edu

Submitted: May 27, 2014
Accepted: June 14, 2014

Citation: Lee C, Wallingford JB, Gross JM. Cluap1 is essential for ciliogenesis and photoreceptor maintenance in the vertebrate eye. *Invest Ophthalmol Vis Sci*. 2014;55:4585–4592. DOI:10.1167/iovs.14-14888

Purpose. To identify the mutation and cell biological underpinnings of photoreceptor defects in zebrafish *au5* mutants.

Methods. Whole genome sequencing and SNP mapping were used to determine the genomic interval that harbors the *au5* mutation. A candidate mutation was cloned and sequenced, and mRNA rescue used to validate that the affected gene was correctly identified. In situ hybridization, immunohistochemistry, and confocal imaging were used to determine the effects on photoreceptor development and maintenance in mutant retinae, and to determine if ciliogenesis or cilia-dependent development was affected in mutant embryos. Expression of tagged proteins and high-speed in vivo confocal imaging was used to quantify intraflagellar transport (IFT) and IFT particle localization within multiciliated cells of the *Xenopus* epidermis.

Results. The *au5* mutants possess a nonsense mutation in *cluap1*, which encodes a component of the IFT machinery. Photoreceptor defects result from degeneration of photoreceptors, and defects in ciliogenesis precede degeneration. Cilia in the olfactory pit are absent, and left-right heart positioning is aberrant, consistent with a role for cluap1 during ciliogenesis and cilia-dependent development. High-speed in vivo imaging demonstrates that cluap1 undergoes IFT and that it moves along the cilium bidirectionally, with similar localization and kinetics as IFT20, an IFT-B complex component.

Conclusions. We identified a novel mutation in *cluap1* and determined that photoreceptor maintenance is dependent on cluap1. Imaging data support a model in which cluap1 is a component of the IFT-B complex, and cilia formation requires cluap1 function. These data may provide new insights into the mechanism of photoreceptor degeneration in retinal ciliopathies.

Keywords: zebrafish, cluap1, photoreceptor degeneration, cilia

Photoreceptor degeneration is the major cause of human adult blindness and it results from the progressive dysfunction and eventual death of photoreceptor cells. In numerous instances, this disorder is linked to genetic mutations and more than 200 genes are implicated in photoreceptor degeneration (https://sph.uth.edu/retnet/). Approximately one-third of these known photoreceptor degeneration genes are associated with ciliary transport defects.[1–3]

Vertebrate photoreceptor cells have a unique morphology, which consists of several distinct regions: the outer segment, the inner segment, the nuclear region, and the synapse. Although outer segments are enriched with proteins and membrane required for phototransduction, they lack ribosomes, and thus, development and maintenance of the outer segment requires delivery of cellular components from the cell body. This delivery occurs through the connecting cilium, a narrow constriction elaborated from the primary cilium and connecting the outer segment and inner segment. Defects of cilia structure or function in photoreceptors result in disruption of ciliary trafficking and ultimately lead to photoreceptor degeneration.[2,3] Indeed, ciliopathies are an emerging class of human diseases and many are associated with progressive blindness.[1–3]

Rapid transport and recycling of proteins and membranes in photoreceptor cells depends on active intraflagellar transport (IFT), a key transport system for movement of cargo within cilia.[4] Intraflagellar transport involves the bidirectional motility of a multisubunit protein complex, called the IFT particle, which consists of two major complexes: IFT-A required for retrograde movement and IFT-B required for anterograde movement. Intraflagellar transport core proteins and IFT-associated proteins are necessary for cilia assembly, maintenance, and signaling, and collectively, they are critical for survival of photoreceptors. Numerous genetic studies in mice and zebrafish have shown that defects associated with many of these IFT proteins lead to photoreceptor degeneration.[5–10] However, several IFT components still remain to be identified and detailed cellular functions for many IFT proteins are unknown.

Clusterin-associated protein 1 (Cluap1) has been identified as a component of the IFT machinery. Initially identified from human cancer studies, Cluap1 was reported to localize to the nucleus and is upregulated in several cancers.[11,12] Moreover,

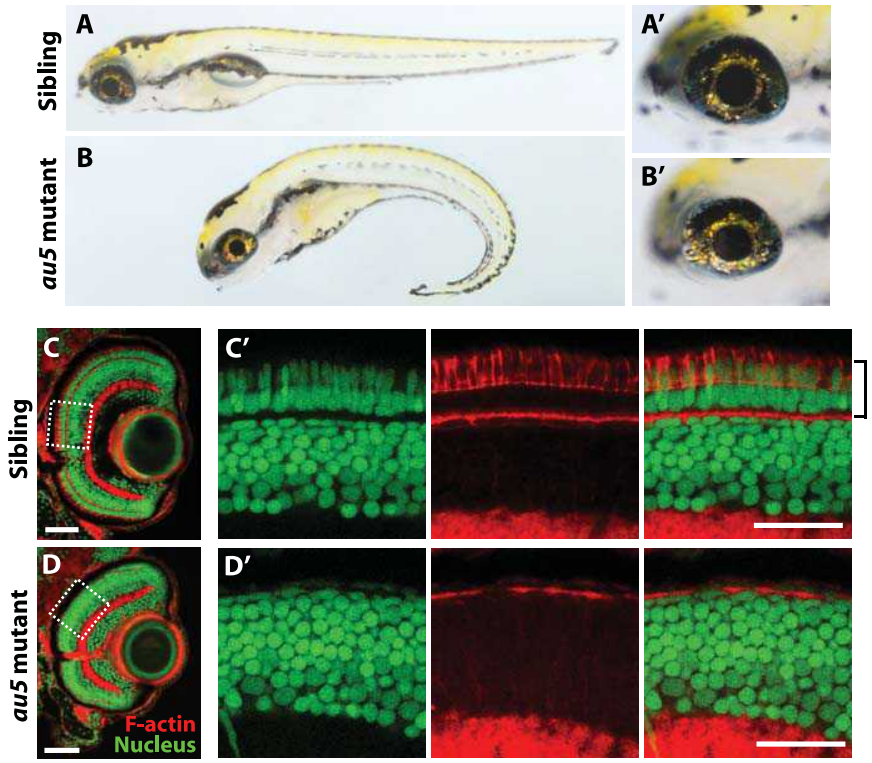

Figure 1. *au*^{5} mutants possess photoreceptor defects. Whole embryo views of wild-type sibling (**A**) and *au*^{5} mutant (**B**) at 7 dpf. *au*^{5} mutants possess a ventral body curvature. (**A′**, **B′**) High-magnification zoom of (**A**) and (**B**) showing mild microphthalmia in *au*^{5} mutants. (**C**, **D**) Cross-section views of wild-type (**C**) and *au*^{5} (**D**) retinas at 7 dpf stained with phalloidin (*red*) and Sytox-Green (*green*). *au*^{5} mutants possess photoreceptor defects when compared with their wild-type siblings. (**C′**) and (**D′**) are high-magnification views of the photoreceptor layer from the boxed in regions of (**C**) and (**D**). Photoreceptor layer is marked by a black bracket in (**C′**). *Scale bars*: 50 μm (**C**, **D**), 20 μm (**C′**, **D′**).

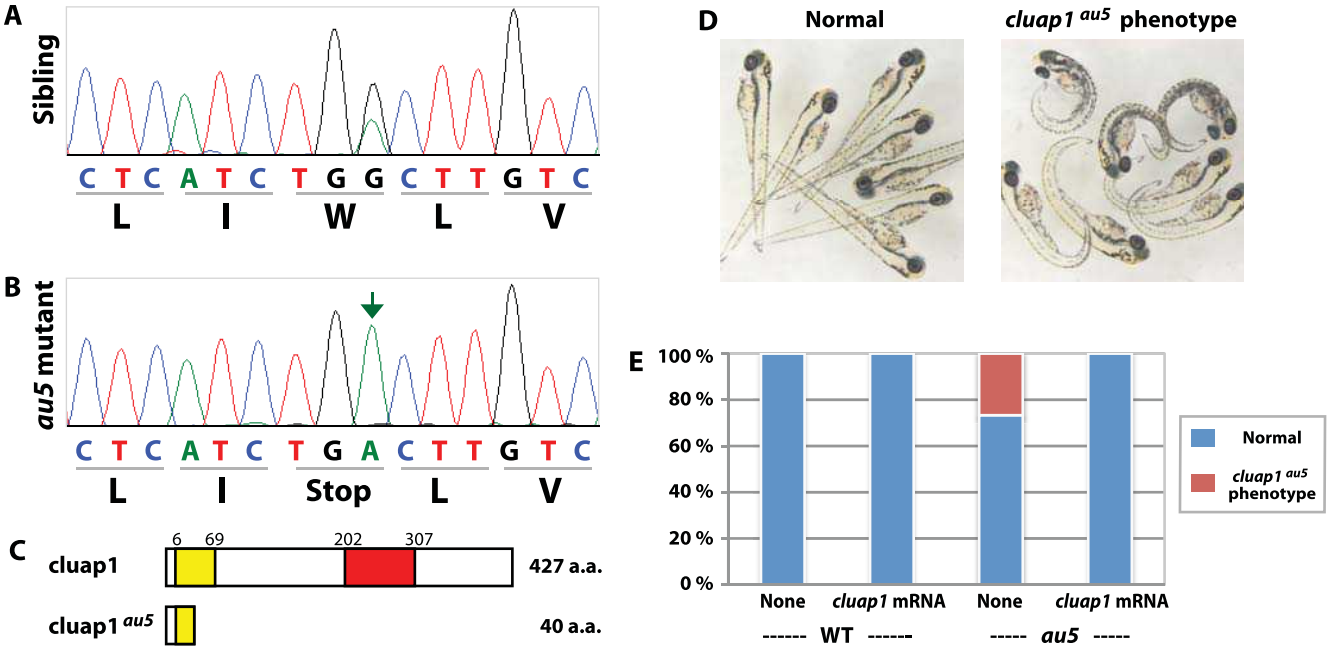

Figure 2. *au*^{5} mutants possess a premature stop codon in *cluap1*. (**A**, **B**) Sequencing results of *cluap1* from phenotypically wild-type siblings (**A**) and *au*^{5} mutants (**B**). *au*^{5} mutants possess a G-to-A transition mutation in *cluap1* (*arrow*) that generates a premature stop codon at amino acid 41 (W41X). (**C**) Schematic of wild-type cluap1 protein and cluap1^{au5}. *Yellow* and *red boxes* represent the predicted NN-CH domains of cluap1, a divergent N-terminal calponin homology (CH)-like domain (6 amino acids (a.a.)–69 a.a.) and coiled-coil box domain (202 a.a.–307 a.a.), respectively. (**D**) Examples of normal and *au*^{5} mutant phenotype at 3 dpf. (**E**) Graph depicting proportion of embryos with phenotypes shown in (**D**). The *au5* mutant phenotype is rescued by injection of *cluap1* mRNA. Uninjected embryos of wild-type ($n = 50$), *cluap1* mRNA injected embryos of wild-type ($n = 47$), uninjected embryos of *au5* ($n = 45$) and *cluap1* mRNA injected embryos of *au5* ($n = 40$).

Investigative Ophthalmology & Visual Science

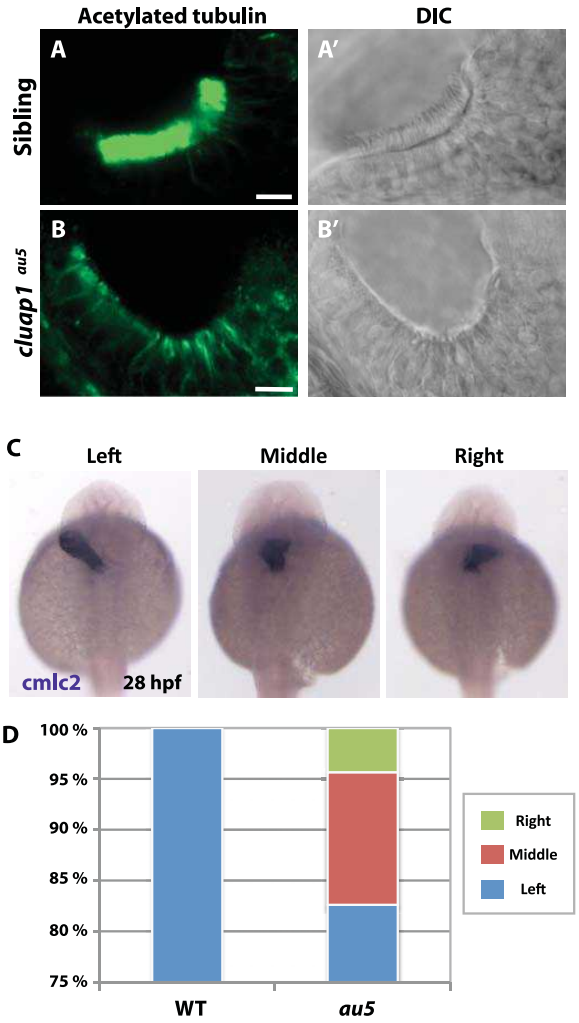

FIGURE 3. *cluap1*^{au5} mutants possess defects in ciliogenesis and cilia-dependent developmental processes. (**A**, **B**) Olfactory pit cilia marked by acetylated alpha tubulin antibody at 3 dpf. When compared to phenotypically wild-type siblings (**A**, **A′**), no cilia are detected in the olfactory pits of *cluap1*^{au5} mutants (**B′**). *Scale bars*: 10 μm. (**C**) Heart tube position determined by *cmlc2* expression 28 hpf. Dorsal views. (**D**) Quantification of the proportion of embryos with left, middle/none, and right heart tube position. The heart of all wild-type embryos ($n = 52$) is on the left side. In clutches of *cluap1*^{au5} embryos ($n = 46$), heart position is defective, with 13.0 % in the middle and 4.34 % on the right.

loss-of-function mutations in *cluap1* (previously known as *qilin*) result in ciliopathy-related phenotypes, such as kidney cysts and photoreceptor defects, in zebrafish.[13,14] *Cluap1*$^{-/-}$ mice have cilia defects, and Cluap1 protein is detected in primary cilia.[15,16] Likewise, mutation of *dyf-3*, the *Caenorhabditis elegans* homolog of *cluap1*, results in morphological abnormality in sensory cilia structure,[17] and a DYF-3::GFP fusion protein undergoes IFT along sensory cilia with a similar velocity to other IFT particles, suggesting that Cluap1 is associated with the IFT complex.[18] Although Cluap1 protein has been localized to mammalian cilia,[15,16] directed IFT of Cluap1 has never been demonstrated in a vertebrate. Moreover, although loss of cluap1 is associated with ocular anomalies,[13] the root cause of these defects is not defined.

In this study, we have characterized the zebrafish *au5* mutant,[23] which harbors a novel mutation in *cluap1*. We show that *cluap1* mutants possess normal development of photoreceptors, but this is followed by progressive degeneration associated with defective cilia. In addition, using high-speed live imaging, we show that Cluap1 travels together with IFT particles, demonstrating that Cluap1 is an IFT particle subunit in vertebrates. These data may provide new insights into the mechanism of photoreceptor degeneration in retinal ciliopathies.[3,19]

Materials and Methods

Animals

Zebrafish and *Xenopus laevis* were maintained as described.[20–22] All protocols used within this study were approved by the Institutional Animal Care and Use Committee of The University of Texas at Austin and conform to the ARVO Statement for the Use of Animals in Ophthalmic and Vision Research. The allele used in this study: *cluap1*^{au5}.[23]

Mutant Cloning

au5 heterozygous carriers (AB background) were outcrossed with wild-type TU fish to generate a mapping line. Heterozygous AB/TU carriers of the *au5* mutation were identified and then incrossed to generate homozygous mutant embryos. Fifty mutant zebrafish embryos from four parental pairs were collected, genomic DNA was isolated (DNeasy Blood & Tissue Kit; Qiagen, Valencia, CA, USA), and 1 μg was used for Illumina sequencing at the University of Texas Genomic Sequencing and Analysis Facility. On an Illumina HiSequation 2000 machine (Illumina, San Diego, CA, USA), 150 million paired-end 100-bp sequences were generated for an average genome coverage of 19X. To identify putative mutations, sequencing reads were analyzed using the BSFseq mapping pipeline on MegaMapper (Megason Lab, Harvard Medical School, Boston, MA, USA).[24] Candidate single nucleotide polymorphisms (SNPs) were confirmed by cDNA sequencing.

mRNA Synthesis and Injection

Wild-type *cluap1* open reading frame was cloned from zebrafish cDNA and inserted into pCS10R and pCS10R-GFP vectors for mRNA synthesis. Capped, poly-adenylated *cluap1* and *cluap1-GFP* were synthesized via a mMESSAGE mMACHINE SP6 Transcription Kit (Life Technologies, Grand Island, NY, USA). For mRNA rescue experiments, 100 pg *cluap1* mRNA was injected into one-cell stage zebrafish embryos. For *Xenopus* experiments, 200 pg *cluap1-GFP*, 150 pg *RFP-IFT20*, and 150 pg *GFP-IFT20* [25] were injected into two ventral cells of four-cell stage embryos.

Immunofluorescence and Whole-Mount In Situ Hybridization

Immunostaining in zebrafish cryosections was performed as described.[26] All antibodies were used at 1:200 dilutions. Primary antibodies were mouse monoclonal anti-acetylated tubulin (T7451; Sigma-Aldrich Corp., St. Louis, MO, USA), anti-zpr1 (ZIRC), and anti-zpr3 (ZIRC). Secondary antibodies were Cy2 or Cy3-conjuated goat anti-mouse (Jackson, West Grove, PA, USA). Phalloidin (Alexa Fluor 488 or 555, Invitrogen, Grand Island, NY, USA) and Sytox-Green were applied to sections to stain F-actin and DNA, respectively. In situ hybridizations were performed as described.[27] For *cmlc2* probe synthesis, a partial cDNA fragment of *cmlc2* was cloned by RT-PCR using primers, 5′-tgtatttaggaggctctgggtgtc-3′ and 5′-ctgctgatgtgaatgttgaactgg-3′.

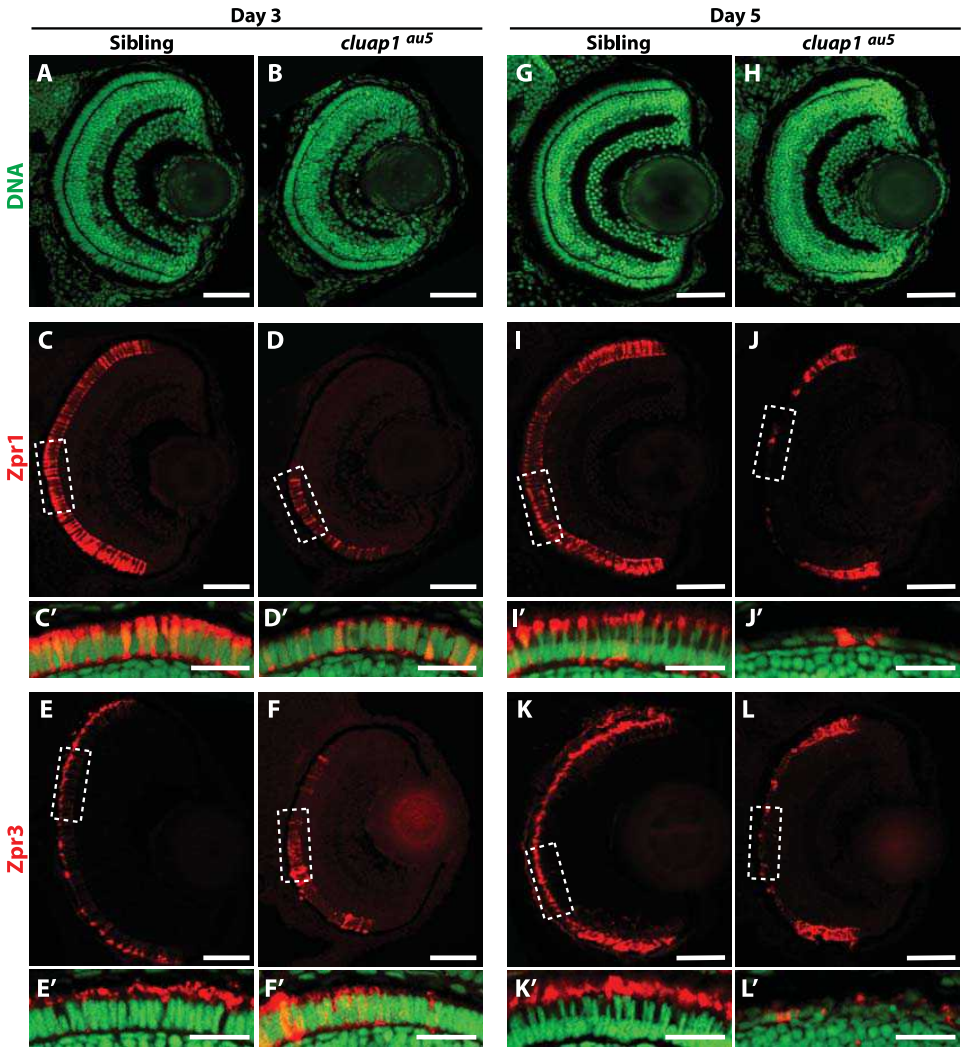

Figure 4. Photoreceptor defects in *cluap1*^{au5} mutants result from degeneration. Transverse sections of zebrafish retinae immunostained for Zpr-1 (a green-red cone cell marker, *red*) or Zpr-3 (a rod cell marker, *red*) and Sytox-Green (DNA, *green*) at 3 dpf (**A–F**) and 5 dpf (**G–L**). *Dashed boxes* in (**C–F**) and (**I–L**) indicate regions from which high-magnification views of the photoreceptor layers are presented in (**C′–F′**) and (**I′–L′**), respectively. Photoreceptor cells expressing Zpr-1 and Zpr-3 are detected at 3 dpf in *cluap1*^{au5} mutants, but by 5 dpf, these have degenerated in the central retina. *Scale bars*: 50 μm (**A–L**), 20 μm (**C′–L′**).

Imaging and Image Analysis

Confocal imaging of cryosections was performed on either a Zeiss LSM5 Pascal or LSM 700 microscope (LSM 5LIVE; Zeiss, Thornwood, NY, USA). High-speed in vivo imaging of IFT was performed as described[25] on a Zeiss LSM 5LIVE microscope. Intraflagellar transport velocities were measured using LSM 5LIVE duoScan software. Whole embryo images were captured on a Leica MZ16FA stereomicroscope (Leica, Buffalo Grove, IL, USA), mounted with a DFC480 digital camera.

Results

au^5 Mutants Possess Photoreceptor Defects

au^5 mutants were identified in a forward genetic screen for embryos possessing morphological defects in eye development, and were identified based on a photoreceptor phenotype.[23] *au*^{5} mutation is recessive, fully penetrant, and embryonic lethal by 10 to 12 days post fertilization (dpf). *au*^{5} mutant embryos do not inflate their swim bladder. Mutant embryos present with a ventral curve to their body axis (Figs. 1A, 1B), which appears at approximately 1.5 dpf. Because of this curvature, mutants are easily distinguished from phenotypically wild-type siblings by 2 dpf. Mutants are also slightly microphthalmic at 3 dpf (Fig. 2D) and 5 dpf (Fig. 1B). Analyzing retinal development at 7 dpf in *au*^{5} mutants revealed a complete absence of photoreceptors in the central retina (Figs. 1C, 1D).

au^5 Mutant Phenotypes Result From a Nonsense Mutation in *cluap1*

To identify the gene mutated in *au*^{5}, we used next-generation sequencing and SNP mapping, generating 19X average genome-wide sequencing coverage. Using the MegaMapper analysis pipeline,[24] a 6-megabase window was identified on chromosome 24 that was predicted to harbor the mutation (Supplementary Fig. S1). Within this window, a G-to-A transition mutation at nucleotide 123 of the *cluap1* coding sequence was identified (Figs. 2A, 2B). This mutation generates

Investigative Ophthalmology & Visual Science

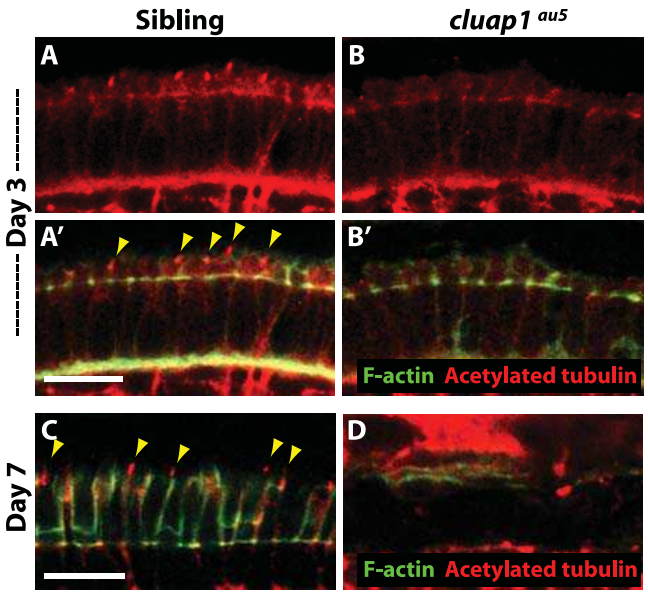

FIGURE 5. Ciliogenesis defects precede photoreceptor degeneration in *cluap1*^{au5} mutant photoreceptor cells. Transverse sections from wild-type and *cluap1*^{au5} mutant retinae immunostained with an acetylated tubulin antibody (*red*) and phalloidin (*green*) to detect cilia and F-actin in photoreceptor outer segments, respectively. (**A**–**B**′) Photoreceptors of 3 dpf and (**C**, **D**) 7 dpf. Cilia are lacking in *cluap1*^{au5} mutant photoreceptors (**B**, **D**) when compared with phenotypically wild-type siblings (**A**, **C**). *Yellow arrowheads* indicate cilia in the photoreceptors. *Scale bars*: 10 μm.

a premature stop codon at amino acid 41 (Trp41Stop) of cluap1, truncating the protein by approximately 90% (Fig. 2C).

To confirm that this is the causative mutation in *au*^{5} mutants, we performed an mRNA rescue experiment by injecting full-length wild-type *cluap1* into *au*^{5} embryos. Overexpression of *cluap1* did not affect development of wild-type embryos, and the mutant phenotype was rescued in all injected embryos (Figs. 2D, 2E). Thus, we conclude that *au*^{5} possesses a mutation in *cluap1* and hereafter refer to this mutant as *cluap1*^{au5}.

Cluap1 is has been previously associated with ciliogenesis in mice and fish.[13,15,16] As further evidence that the identified mutation in *cluap1* was causative for the *au*^{5} phenotypes, we examined ciliogenesis and cilia-related developmental defects. The olfactory epithelium of zebrafish is normally ciliated, and we found that olfactory epithelial cells lacked cilia in *cluap1*^{au5} mutants (Figs. 3A, 3B). Moreover, although Cluap1 has been shown to be required for nodal ciliogenesis and left/right asymmetry in mice,[16] its role in in the zebrafish left/right patterning is not known. We performed whole-mount in situ hybridization using *cardiac myosin light chain 2* (*cmlc2*) as a marker for the position of the heart tube.[28] At 28 hours post fertilization, the heart tube is positioned to the left side of wild-type embryos (Figs. 3C, 3D). However, in embryos derived from *cluap1*^{au5} heterozygous incrosses, heart tube position was randomized, with 13% of embryos possessing *cmlc2* expression in the middle of the heart field, and 4.3% of embryos on the right side (Figs. 3C, 3D). Given that 25% of embryos from such crosses are *cluap1*^{au5} mutants, these data demonstrate that left-right asymmetry was defective in *cluap1*^{au5} mutants. Taken together, these data demonstrate that *cluap1*^{au5} mutants display cilia defects, consistent with a role for cluap1 in ciliogenesis.[13,15,16]

Progressive Photoreceptor Degeneration in *cluap1*^{au5} Mutants

A previous study of *cluap1* in zebrafish revealed an absence of photoreceptors at 5 dpf, but the cause of this defect has not been explored.[13] Because human ciliopathies are frequently associated with retinal degeneration,[2,29,30] we hypothesized that the photoreceptor defects observed in *cluap1*^{au5} mutants might be the result of degeneration, rather than defects in specification or differentiation.

To test this hypothesis, we analyzed photoreceptor cell formation at the early stages of retinal development. In zebrafish, differentiation of photoreceptors initiates at approximately 2 dpf, with the photoreceptor layer becoming morphologically distinct by 3 dpf, at which point photoreceptors have formed obvious outer segments and become functional.[31] At 3 dpf, the retina in *cluap1*^{au5} mutants was well formed, and an outer nuclear layer was present (Figs. 4A, 4B). However, using zpr3 and zpr1 as immunohistochemical markers for rods and red-green cones, respectively, revealed that whereas these were present in the *cluap1*^{au5} mutant retina, there were fewer photoreceptors expressing these proteins, and those that did possessed markedly shorter outer segments (Figs. 4C–F). By 5 dpf, the photoreceptor layer in *cluap1*^{au5} mutants was almost completely absent from the central retina, and photoreceptors were present only in the peripheral retina, near the ciliary marginal zone, where photoreceptors are continually generated (Figs. 4G–L). These data suggest that in *cluap1*^{au5} mutants, photoreceptor cells are impaired in their ability to form outer segments, and that they ultimately degenerate.

Ciliogenesis Defects Precede Photoreceptor Defects in *cluap1*^{au5} Mutants

Previous studies have demonstrated that Cluap1 is required for cilia assembly and maintenance,[13,15,16] but the development of

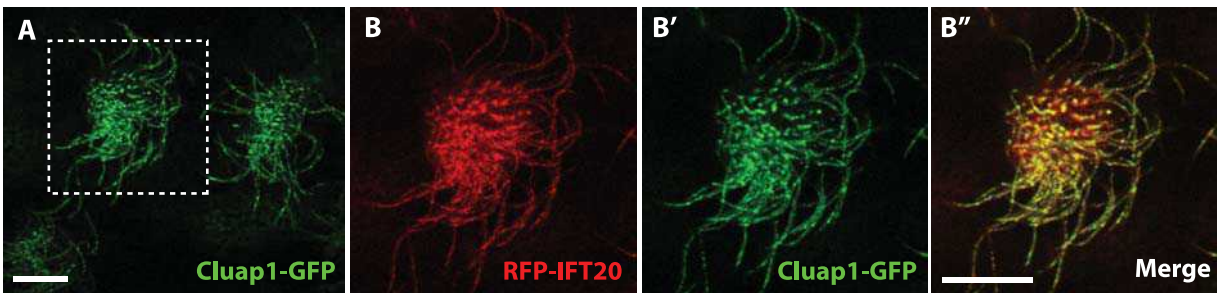

FIGURE 6. Cluap1-GFP localizes to the axoneme and basal body of cilia of *Xenopus* multiciliated cells. (**A**) Cluap1-GFP is detected at the basal body and axoneme of cilia emanating from multiciliated cells on the surface of *Xenopus* embryo (stage 25). (**B**–**B**″) High-magnification view of *dashed box* in (**A**). Cluap1-GFP colocalizes with RFP-IFT20 (Cluap1-GFP, *green*; RFP-IFT20, *red*). *Scale bars*: 10 μm.

Investigative Ophthalmology & Visual Science

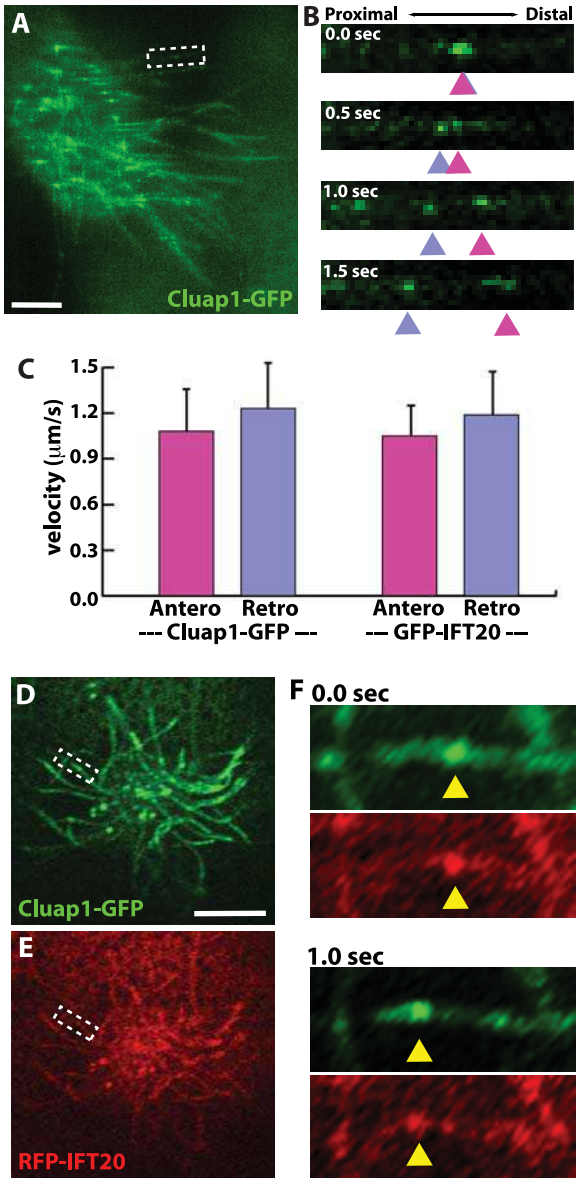

Figure 7. Cluap1-GFP undergoes IFT with a similar velocity to IFT-20. (**A**) Still image from a time-lapse video of Cluap1-GFP in *Xenopus* multiciliated cell (stage 25). *Scale bar*: 5 μm. (**B**) High-magnification view of *boxed region* in (**A**). Time-lapse images of Cluap1-GFP movement along the axoneme demonstrate that Cluap1-GFP undergoes both anterograde and retrograde IFT. (**C**) Graph depicting the velocities of Cluap1-GFP and GFP-IFT20. Cluap1 moves with a similar velocity to IFT20 in both the anterograde and retrograde directions. Mean velocities ± SD are 1.076 ± 0.28 μm/s ($n = 46$ from 8 cells) for Cluap1-GFP anterograde, 1.23 ± 0.30 μm/s ($n = 68$ from 8 cells) for Cluap1-GFP retrograde, 1.05 ± 0.20 μm/s ($n = 27$ from 9 cells) for GFP-IFT20 anterograde and 1.19 ± 0.29 μm/s ($n = 53$ from 9 cells) for GFP-IFT20 retrograde. (**D**, **E**) Still images of time-lapse movies showing Cluap1-GFP (**D**) and RFP-IFT20 (**E**) localization in cilia. *Scale bar*: 10 μm. (**F**) High-magnification view of boxed regions in (**D**, **E**). Time-lapse images of Cluap1-GFP and RFP-IFT20 movement along the axoneme support that Cluap1-GFP and RFP-IFT20 are transported in the same IFT particle.

connecting cilia has yet to be investigated directly in cluap1-deficient photoreceptors in any animal. Because we observed that photoreceptor degeneration was progressive over time, we were able to examine connecting cilia directly in *cluap1*^{au5} mutants at 3 dpf. Using acetylated α-tubulin immunostaining, cilia were easily detected in photoreceptor cells of wild-type siblings (Fig. 5A, arrowheads). In contrast, although photoreceptor cells are present at 3 dpf in *cluap1*^{au5} mutants (Fig. 5B), no cilia were detected in these photoreceptor cells (Fig. 5B). Similarly, no cilia were detected at 7 dpf in *cluap1*^{au5} mutants, despite obvious cilia on the photoreceptors of wild-type siblings (Figs. 5C, 5D). Thus, loss of cilia in precedes photoreceptor degeneration in *cluap1*^{au5} mutants.

Cluap1 Undergoes IFT in a Vertebrate

In *C. elegans*, Cluap1/DYF-3 is required for normal IFT, and Cluap1 itself undergoes bidirectional transport with similar velocity as other IFT-B complex particles.[18] However, the transport mechanisms of IFT particles in *C. elegans* differ from those in vertebrates,[32,33] and vertebrate Cluap1 has been variably reported to localize either along axonemes[15] or to the tips and base of cilia.[16] To directly analyze the localization and dynamics of Cluap1 in a vertebrate system, we turned to the muticiliated cells of the *Xenopus* epidermis, which provide an excellent system in which to examine IFT by live imaging in a vertebrate.[25,34–36]

We expressed Cluap1-GFP and observed that it localized to both the basal body and the axoneme in a pattern similar to IFT20, a subunit of the IFT-B complex (Fig. 6). Moreover, high-speed in vivo imaging showed that Cluap1-GFP moved bidirectionally along the axoneme (Fig. 7B), and its velocity in both the anterograde and retrograde direction was similar to that of IFT20 (Fig. 7C). Finally, from high-speed, two-color imaging, we could observe that Cluap1-GFP and RFP-IFT20 colocalized and were cotransported in the same particles (Figs. 7D–F). These data support a model in which vertebrate Cluap1 undergoes IFT as part of the IFT-B complex in vertebrate cilia.[13,15,37]

Discussion

Ciliopathies are human genetic disorders caused by mutations in genes regulating cilia formation or function.[38] In many cases, ciliopathies involve a wide range of clinical features, and these include defects in the retina, as well as other organ systems. Syndromic ciliopathies that present with photoreceptor involvement include Alstrom syndrome (MIM 203800), Bardet-Biedl syndrome (MIM 209900), Joubert syndrome (MIM 213300), Meckel-Gruber syndrome (MIM 249000), Senior-Loken syndrome (MIM 266900), Usher syndrome (MIM 276901), and nephronophthisis. Nonsyndromic retinal ciliopathies include retinitis pigmentosa (MIM 268000), cone-rod dystrophy (MIM 120970), and Leber's congenital amaurosis (MIM 204000).[2,39] Vertebrate animal models have become powerful tools through which the relationships between the clinical features observed in ciliopathy patients, and the genetic and molecular underpinnings of disease can be elucidated.[2,5,9,40–46]

In this study, we identify a zebrafish model that may provide novel insights into the genetic basis of ciliopathic blindness. We report on a novel mutation in the zebrafish *cluap1* gene, and describe ciliogenesis defects in *cluap1*^{au5} mutants that are similar to those observed in other regions of the zebrafish embryo,[13] as well as in *Cluap1* knockout mice[15,16] and *C. elegans* dyf-3 mutants.[17] Photoreceptor defects have been reported in *cluap1* mutant zebrafish, but no further analysis of this phenotype has been reported.[13] Here, we show directly for the first time that ciliogenesis is defective in the photoreceptors of *cluap1*^{au5} mutants, and we show that these defects precede a progressive degeneration of photoreceptors. Photoreceptor degeneration resulting from loss of cluap1

function proceeds in a central to peripheral pattern, and this is consistent with the central retinal photoreceptors being the oldest and first affected, whereas those more peripheral are younger, having differentiated later. Details like these on the etiology of the retinal pathology in *cluap1*^{au5} mutants are significant for understanding the pathogenesis of ciliopathic eye defects. For example, although most ciliopathies involve cilia defects in photoreceptors,[2,39] a new ciliopathy has recently been described with ciliogenesis defects in retinal precursors and not in photoreceptors.[47,48]

Interestingly, this new ciliopathy results from mutation in intestinal cell kinase, which in turn controls the localization of IFT proteins,[47] and our data provide new details on the link between IFT and cluap1. Cluap1 mutants in a variety of systems possess phenotypes that resemble those in mutants for other IFT-B components, and these include defects in ciliogenesis and defective Shh signaling.[15,49–51] In mice, Cluap1 binds to IFT88, an IFT-B component, and not IFT140, an IFT-A component,[37] and a recent proteomic screen identified Cluap1 as an integral component of the IFT-B complex.[52] Moreover, according to sequence profile-to-profile analysis and structure analysis, Cluap1 shares overall protein architecture with some IFT-B components.[53] Finally, Dyn-3::GFP undergoes IFT in *C. elegans*,[18] but there are key differences in the mechanisms driving IFT in *C. elegans* and vertebrates (e.g., Refs. 32 and 33), and the previous reports of Cluap1 localization in vertebrate cilia have not been consistent.[15,16] Our finding here, using high-speed in vivo imaging, reveals for the first time that Cluap1-GFP undergoes bidirectional IFT in vertebrate cilia and colocalizes with IFT20, an IFT-B complex protein. These data provide direct support for a role for Cluap1 in the IFT-B complex in vertebrates, and help to elucidate the etiology of ciliopathic photoreceptor degeneration.

Acknowledgments

We thank members of the Gross and Wallingford laboratories for comments on this study, and Sallie Ford for technical assistance.

Supported by National Institutes of Health/National Eye Institute Grant R21-EY22770 (JMG). JBW is an early career scientist of the Howard Hughes Medical Institute and work in his laboratory is funded by grants from the National Institute of General Medical Sciences and the National Heart, Lung, and Blood Institute. Zebrafish antisera were obtained from Zebrafish International Resource Center, which is supported by National Institutes of Health–National Center for Research Resources Grant P40 RR012546.

Disclosure: **C. Lee**, None; **J.B. Wallingford**, None; **J.M. Gross**, None

References

1. Wright AF, Chakarova CF, Abd El-Aziz MM, Bhattacharya SS. Photoreceptor degeneration: genetic and mechanistic dissection of a complex trait. *Nat Rev Genet*. 2010;11:273–284.
2. Estrada-Cuzcano A, Roepman R, Cremers FP, den Hollander AI, Mans DA. Non-syndromic retinal ciliopathies: translating gene discovery into therapy. *Hum Mol Genet*. 2012;21:R111–R124.
3. Wheway G, Parry DA, Johnson CA. The role of primary cilia in the development and disease of the retina. *Organogenesis*. 2014;10:69–85.
4. Ishikawa H, Marshall WF. Ciliogenesis: building the cell's antenna. *Nat Rev Mol Cell Biol*. 2011;12:222–234.
5. Sukumaran S, Perkins BD. Early defects in photoreceptor outer segment morphogenesis in zebrafish ift57, ift88 and ift172 intraflagellar transport mutants. *Vision Res*. 2009;49:479–489.
6. Tsujikawa M, Malicki J. Intraflagellar transport genes are essential for differentiation and survival of vertebrate sensory neurons. *Neuron*. 2004;42:703–716.
7. Pazour GJ, Baker SA, Deane JA, et al. The intraflagellar transport protein, IFT88, is essential for vertebrate photoreceptor assembly and maintenance. *J Cell Biol*. 2002;157:103–113.
8. Hudak LM, Lunt S, Chang CH, et al. The intraflagellar transport protein ift80 is essential for photoreceptor survival in a zebrafish model of jeune asphyxiating thoracic dystrophy. *Invest Ophthalmol Vis Sci*. 2010;51:3792–3799.
9. Krock BL, Perkins BD. The intraflagellar transport protein IFT57 is required for cilia maintenance and regulates IFT-particle-kinesin-II dissociation in vertebrate photoreceptors. *J Cell Sci*. 2008;121:1907–1915.
10. Beales PL, Bland E, Tobin JL, et al. IFT80, which encodes a conserved intraflagellar transport protein, is mutated in Jeune asphyxiating thoracic dystrophy. *Nat Genet*. 2007;39:727–729.
11. Ishikura H, Ikeda H, Abe H, et al. Identification of CLUAP1 as a human osteosarcoma tumor-associated antigen recognized by the humoral immune system. *Int J Oncol*. 2007;30:461–467.
12. Takahashi M, Lin YM, Nakamura Y, Furukawa Y. Isolation and characterization of a novel gene CLUAP1 whose expression is frequently upregulated in colon cancer. *Oncogene*. 2004;23:9289–9294.
13. Li J, Sun Z. Qilin is essential for cilia assembly and normal kidney development in zebrafish. *PLoS One*. 2011;6:e27365.
14. Sun Z, Amsterdam A, Pazour GJ, Cole DG, Miller MS, Hopkins N. A genetic screen in zebrafish identifies cilia genes as a principal cause of cystic kidney. *Development*. 2004;131:4085–4093.
15. Pasek RC, Berbari NF, Lewis WR, Kesterson RA, Yoder BK. Mammalian Clusterin associated protein 1 is an evolutionarily conserved protein required for ciliogenesis. *Cilia*. 2012;1:20.
16. Botilde Y, Yoshiba S, Shinohara K, et al. Cluap1 localizes preferentially to the base and tip of cilia and is required for ciliogenesis in the mouse embryo. *Dev Biol*. 2013;381:203–212.
17. Murayama T, Toh Y, Ohshima Y, Koga M. The dyf-3 gene encodes a novel protein required for sensory cilium formation in *Caenorhabditis elegans*. *J Mol Biol*. 2005;346:677–687.
18. Ou G, Qin H, Rosenbaum JL, Scholey JM. The PKD protein qilin undergoes intraflagellar transport. *Curr Biol*. 2005;15:R410–R411.
19. Boldt K, Mans DA, Won J, et al. Disruption of intraflagellar protein transport in photoreceptor cilia causes Leber congenital amaurosis in humans and mice. *J Clin Invest*. 2011;121:2169–2180.
20. Westerfield M. *The Zebrafish Book: A Guide for the Laboratory use of Zebrafish (*Danio rerio*)*. Eugene, OR: University of Oregon Press; 1995.
21. Kimmel CB, Ballard WW, Kimmel SR, Ullmann B, Schilling TF. Stages of embryonic development of the zebrafish. *Dev Dyn*. 1995;203:253–310.
22. Sive HLG, Harland, RM. *Early Development of* Xenopus laevis*: A Laboratory Manual*. Cold Spring Harbor, NY: Cold Spring Harbor Laboratory Press; 2000.
23. Lee J, Cox BD, Daly CM, et al. An ENU mutagenesis screen in zebrafish for visual system mutants identifies a novel splice-acceptor site mutation in patched2 that results in Colobomas. *Invest Ophthalmol Vis Sci*. 2012;53:8214–8221.
24. Obholzer N, Swinburne IA, Schwab E, Nechiporuk AV, Nicolson T, Megason SG. Rapid positional cloning of zebrafish mutations by linkage and homozygosity mapping using whole-genome sequencing. *Development*. 2012;139:4280–4290.

25. Brooks ER, Wallingford JB. Control of vertebrate intraflagellar transport by the planar cell polarity effector Fuz. *J Cell Biol*. 2012;198:37–45.
26. Uribe RA, Gross JM. Immunohistochemistry on cryosections from embryonic and adult zebrafish eyes. *CSH Protoc*. 2007; 2007;pdb.prot4779.
27. Jowett T, Lettice L. Whole-mount in situ hybridizations on zebrafish embryos using a mixture of digoxigenin- and fluorescein-labelled probes. *Trends Genet*. 1994;10:73–74.
28. Yelon D, Horne SA, Stainier DY. Restricted expression of cardiac myosin genes reveals regulated aspects of heart tube assembly in zebrafish. *Dev Biol*. 1999;214:23–37.
29. Novarino G, Akizu N, Gleeson JG. Modeling human disease in humans: the ciliopathies. *Cell*. 2011;147:70–79.
30. Badano JL, Mitsuma N, Beales PL, Katsanis N. The ciliopathies: an emerging class of human genetic disorders. *Annu Rev Genomics Hum Genet*. 2006;7:125–148.
31. Raymond PA, Barthel LK, Curran GA. Developmental patterning of rod and cone photoreceptors in embryonic zebrafish. *J Comp Neurol*. 1995;359:537–550.
32. Snow JJ, Ou G, Gunnarson AL, et al. Two anterograde intraflagellar transport motors cooperate to build sensory cilia on *C. elegans* neurons. *Nat Cell Biol*. 2004;6:1109–1113.
33. Pan X, Ou G, Civelekoglu-Scholey G, et al. Mechanism of transport of IFT particles in C. elegans cilia by the concerted action of kinesin-II and OSM-3 motors. *J Cell Biol*. 2006;174: 1035–1045.
34. Werner ME, Mitchell BJ. Understanding ciliated epithelia: the power of *Xenopus*. *Genesis*. 2012;50:176–185.
35. Chung MI, Kwon T, Tu F, et al. Coordinated genomic control of ciliogenesis and cell movement by RFX2. *Elife*. 2014;3:e01439.
36. Brooks ER, Wallingford JB. The small GTPase Rsg1 is important for the cytoplasmic localization and axonemal dynamics of intraflagellar transport proteins. *Cilia*. 2013;2:13.
37. Follit JA, Xu F, Keady BT, Pazour GJ. Characterization of mouse IFT complex B. *Cell Motil Cytoskeleton*. 2009;66:457–468.
38. Rachel RA, Li T, Swaroop A. Photoreceptor sensory cilia and ciliopathies: focus on CEP290, RPGR and their interacting proteins. *Cilia*. 2012;1:22.
39. Baker K, Beales PL. Making sense of cilia in disease: the human ciliopathies. *Am J Med Genet C Semin Med Genet*. 2009;151C: 281–295.
40. Duldulao NA, Lee S, Sun Z. Cilia localization is essential for in vivo functions of the Joubert syndrome protein Arl13b/ Scorpion. *Development*. 2009;136:4033–4042.
41. Pretorius PR, Aldahmesh MA, Alkuraya FS, Sheffield VC, Slusarski DC. Functional analysis of BBS3 A89V that results in non-syndromic retinal degeneration. *Hum Mol Genet*. 2011; 20:1625–1632.
42. Sayer JA, Otto EA, O'Toole JF, et al. The centrosomal protein nephrocystin-6 is mutated in Joubert syndrome and activates transcription factor ATF4. *Nat Genet*. 2006;38:674–681.
43. Baye LM, Patrinostro X, Swaminathan S, et al. The N-terminal region of centrosomal protein 290 (CEP290) restores vision in a zebrafish model of human blindness. *Hum Mol Genet*. 2011; 20:1467–1477.
44. Miller KA, Ah-Cann CJ, Welfare MF, et al. Cauli: a mouse strain with an Ift140 mutation that results in a skeletal ciliopathy modelling Jeune syndrome. *PLoS Genet*. 2013;9:e1003746.
45. Lehman JM, Michaud EJ, Schoeb TR, Aydin-Son Y, Miller M, Yoder BK. The Oak Ridge Polycystic Kidney mouse: modeling ciliopathies of mice and men. *Dev Dyn*. 2008;237:1960–1971.
46. Ashe A, Butterfield NC, Town L, et al. Mutations in mouse Ift144 model the craniofacial, limb and rib defects in skeletal ciliopathies. *Hum Mol Genet*. 2012;21:1808–1823.
47. Chaya T, Omori Y, Kuwahara R, Furukawa T. ICK is essential for cell type-specific ciliogenesis and the regulation of ciliary transport. *EMBO J*. 2014;33:1227–1242.
48. Lahiry P, Wang J, Robinson JF, et al. A multiplex human syndrome implicates a key role for intestinal cell kinase in development of central nervous, skeletal, and endocrine systems. *Am J Hum Genet*. 2009;84:134–147.
49. Tran PV, Haycraft CJ, Besschetnova TY, et al. THM1 negatively modulates mouse sonic hedgehog signal transduction and affects retrograde intraflagellar transport in cilia. *Nat Genet*. 2008;40:403–410.
50. Qin J, Lin Y, Norman RX, Ko HW, Eggenschwiler JT. Intraflagellar transport protein 122 antagonizes Sonic Hedgehog signaling and controls ciliary localization of pathway components. *Proc Natl Acad Sci U S A*. 2011;108:1456–1461.
51. Huangfu D, Anderson KV. Cilia and Hedgehog responsiveness in the mouse. *Proc Natl Acad Sci U S A*. 2005;102:11325–11330.
52. Texier Y, Toedt G, Gorza M, et al. Elution profile analysis of SDS-induced subcomplexes by quantitative mass spectrometry. *Mol Cell Proteomics*. 2014;13:1382–1391.
53. Schou KB, Andersen JS, Pedersen LB. A divergent calponin homology (NN-CH) domain defines a novel family: implications for evolution of ciliary IFT complex B proteins. *Bioinformatics*. 2014;30:899–902.

Investigative Ophthalmology & Visual Science